JOURNAL OF MATERIALS SCIENCE 32 (1997) 2207–2213

Formation of opaque films by biomimetic process

E. F. DE SOUZA, F. GALEMBECK*
Institute of Chemistry, University of Campinas, CP 6154, 13083-970, Campinas, SP, Brazil

The preparation of opaque white films with amorphous aluminium polyphosphate, crystalline calcium carbonate and poly(vinyl acetate) latex is described. Film optical properties were characterized by diffuse reflectance spectrophotometry; morphological film features were examined by SEM, TEM, STM and AFM. Domain organization and void formation were detected, with dimensions of the same order of magnitude as the wavelength of visible light and can thus account for the film optical properties. Calcium carbonate consumption was monitored by X-ray diffraction and is assigned to a chemical reaction with aluminium polyphosphate, in which a mixed Al–Ca carbonate–polyphosphate is formed. The process of film opacification is interpreted as a result of dispersion, chemical reaction and orientation of solid inorganic particles within the polymer network during the film drying process. A model is proposed for void formation, based on volume contraction of the swollen inorganic particles, at a stage when their rigid surfaces are bound to the polymeric matrix.

1. Introduction

Mineralized tissues and many other biological materials are biocomposites, produced by cell-mediated processes, in which inorganic particles reinforce a polymer matrix [1, 2]. Compared to synthetic materials, biocomposites have two remarkable characteristics: they are formed by a mineral phase grown within an organic matrix, from common inorganic compounds and have very sophisticated shape, size, orientation and organization of the mineral particles. The structure of biocomposites seems to have a greater influence over the materials characteristics than the bulk components properties.

The fabrication of biocomposites by living systems begins with cellular secretion of a polymeric matrix that is subsequently filled by inorganic, usually crystalline particles produced *in situ* within the matrix and under its control. The formation of amorphous biocomposites is also observed in some cases, for instance in biomaterials containing amorphous carbonates or phosphates. In this case, the organic matrix inhibits crystal nucleation thereby increasing the amorphous phase kinetic stability and controlling particle growth. In oriented biocomposites, the organic matrix controls not only nucleation but also crystal size, morphology and habit, crystallographic structure and orientation during mineral phase growth [1–3].

The initial stage of biomineralization is the construction of an organized reaction environment before mineralization and this is known as supramolecular pre-organization. The organic matrix is the structural component that defines the region to be mineralized, both spatially and temporally. The second stage of biomineralization is the controlled nucleation of inorganic aggregates from aqueous solution. The organic supramolecular system provides a support network with functionalized surfaces that work as templates for inorganic nucleation by a process of interfacial molecular recognition. The structural correspondence between the functional groups of the matrix and the crystallographic lattice dimensions induces the oriented nucleation of a specific face of the crystal. The crystal adopts the habit and orientation specified by the matrix architecture, that are not necessarily the same obtained by spontaneous precipitation from a supersaturated solution [2–5].

The study of biomineralization and related processes may teach us about the extent and nature of interfacial chemistry in organic–inorganic systems. The term "molecular tectonics" was proposed by S. Mann (1993) to describe biomimetic processes of materials synthesis related to the chemical build-up of ordered architectures in organic–inorganic systems. The concepts of supramolecular pre-organization and interfacial molecular recognition borrowed from biological systems may be used to produce, starting from molecular components, the organized systems in nanometric or micrometric scales that are needed to fabricate many advanced materials. These processing strategies based on biology can originate composites with physical, optical, electrical and mechanical properties not obtained by conventional techniques. Presently, the biomimetic approach is centred on the study of processes and properties at the mineral–organic interface, mostly in systems with crystalline inorganic materials and in the production of ceramic films [2, 6–11].

*Author for correspondence.

0022–2461

In this work, we report the preparation of hollow structures with a large light backscattering ability, within films of poly(vinyl acetate) (PVA). These structures are made with the non-crystalline product of the reaction of aluminium polyphosphate ($Al[PO_3]_n$) and calcium carbonate ($CaCO_3$). This has practical interest, because the resulting opaque films work as if they were pigmented, even though they do not contain any usual white, high-refractive index pigment such as rutile. In these opaque films the optical properties are rather the result of a morphogenetic process that can be explained with the help of molecular tectonic concepts.

2. Experimental details

2.1. Aluminium polyphosphate characterization

Aluminium polyphosphate was prepared in kilogram amounts in the Codetec (Campinas) multi-purpose pilot plant, by simultaneous admixture of equal volumes of aqueous solutions of 2 M (PO_3) sodium polyphosphate $(NaPO_3)_n$, 1 M (Al) hydrated aluminium sulphate $Al_2(SO_4)_3 \cdot 12H_2O$ and 0.7 M ammonium hydroxide, within a stirred batch, glass lined reactor with 100 L of total volume. This was equipped with a vertical stirrer and three baffles. The reaction was done at plant (17–27 °C) temperature and atmospheric pressure. At the end of the reaction the suspension of solids obtained was maintained under stirring for 10 min. Then, the product was centrifuged, washed with water and dried for 24 h at 80 °C and then until constant weight, at 140 °C. The dry solids were ground in a two-roll mill to pass a 20-mesh screen and finally were micronized in an air-blast mill, at the Farma Service company (São Paulo).

Phosphorus was determined spectrophotometrically by the molybdenum blue method using a UV/vis Micronal B382 spectrophotometer, with dihydrogen sodium phosphate as the primary standard. Aluminium was determined by complexometric titration with EDTA (ethylene diamine tetra-acetic acid) and sodium was determined by flame photometry using a Micronal B262 flame photometer, with sodium chloride as a standard. The specific weight was measured using a Micromeritics 1305 helium pycnometer.

Transmission electron micrographs (TEM) were obtained using a Zeiss CEM902 microscope fitted with an electron monochromator. Samples examined by TEM were prepared from aqueous dispersions of $Al[PO_3]_n$ and $CaCO_3$, using the non-ionic surfactant ethoxylated nonylphenol (Renex 90) as dispersing agent, by placing one droplet of dispersion directly over the TEM copper grid coated with parlodion/carbon, followed by 24 h drying under air.

2.2. Film preparation and characterization

Films were prepared with a 40% total pigment volume concentration (PVC) and with different ratios of volumetric concentrations of aluminium polyphosphate and calcium carbonate. To prepare the pigment dispersions, $Al[PO_3]_n$ and $CaCO_3$ were weighed and pre-dispersed in distilled water using a shearing mixer ("tissue homogenizer"). This dispersion was added to a definite amount of latex and the mixture was homogenized again using the shearing mixer. The latex–particle dispersion was defoamed for 90 s in a 25 kHz Thornton GA 200 ultrasonic cleaning bath. The films were cast according to the ASTM D 823-87 standard. The dispersion was spread as a paint (using a Microntest device) on glass sheets (5 mm × 100 mm × 100 mm), previously cleaned and dried. The films were air-dried for at least 12 h before applying a second dispersion layer or doing any further analysis.

The thickness of the dry films was measured with a micrometer according to ASTM D 1005-84 standard. The contrast ratio was determined as the ratio between the red light (from a light emission diode) intensity that is reflected by the film placed over a black surface and by the same film placed over a white surface. The opacifying characteristics of the films were further evaluated by measurement of the diffuse reflectance spectrum within the wavelength range from 360 to 740 nm, using a Macbeth Color Eye 2020 instrument. The results were compared with those of a standard film cast using an aqueous dispersion of titanium dioxide (TiO_2) and PVA latex with a 20% pigment volumetric concentration. X-ray diffractograms were obtained using a Zeiss Jena URD-6 diffractometer; CuK_α radiation was generated at 30 kV and 20 mA. For each volumetric ratio of polyphosphate and carbonate we also prepared a standard containing only calcium carbonate at the same original concentration used in the sample film. In the standard films, the volume of polyphosphate was replaced by PVA. All components were weighed to the nearest 0.01 mg. The films were cast directly on the instrument sample holder and examined after 12 h drying under air. Scanning electron micrographs (SEM) and energy dispersive spectrometric (EDS) analysis were performed with a Jeol T300 microscope operating at 20 kV. Samples observed by SEM were detached fractions of a dried film cast over a glass panel, fixed on the sample support and gold coated. Both cast and fracture surfaces were examined. Atomic force and tunnelling images were obtained with a tunnelling/atomic force microscope (AFM/STM) TopoMetrix TMX 2000, using 70 and 7 μm scanners. Pure PVA films cast directly on the instrument sample holder as well as the detached fractions of dried films were examined by AFM. The samples containing polyphosphate, carbonate and PVA observed by STM were detached fractions of dried films cast over a glass panel, fixed on the sample support and gold coated.

3. Results and discussion

The amorphous aluminium polyphosphate contains 10.9% (weight) P, 25.0% Al and less than 0.5% Na. The specific weight of the micronized powder is 2.813 g cm^{-3}.

Table I presents the thickness and the contrast ratio of the films prepared with polyphosphate, carbonate

TABLE I Thickness and contrast ratio of the coating films prepared with polyphosphate, carbonate and PVA

Film	$Al[PO_3]_n/CaCO_3$ ratio	Thickness	Contrast ratio
D1	20:80	51 ± 2	0.865 ± 0.033
D2	30:70	45	0.873
D3	40:60	51	0.873
D4	50:50	43 ± 2	0.786 ± 0.034
D5	60:40	44	0.885
D6	70:30	43	0.889
D7	80:20	47	0.881

and PVA cast over glass panels and air dried. The average thickness of dried one-layer films is 47 μm. The contrast ratio is 0.88 except for films identified as D1 and D4.

Fig. 1 presents the diffuse reflectance spectra of two-layer films D3, D4, and D6, in which the polyphosphate-to-carbonate ratio is varied from 40:60 to 60:40. The films containing polyphosphate, carbonate and PVA have reflectance curves flatter than that containing TiO_2 and do not show any significant absorption bands in near-ultraviolet (UV). The films reflectances are within the 70 to 77% range throughout the wavelength range examined. The standard film of TiO_2 shows reflectances from 80 to 85% at wavelengths above 420 nm, but it has considerable absorption in the near-UV region which reduces its reflectance down to 11–40%. These results are particularly interesting if we consider that the refractive indices of polyphosphate and carbonate are in the range 1.5–1.7, and therefore very close to the refractive index of PVA ($n = 1.47$) and well below that of TiO_2 rutile ($n = 2.6$). It is clear that neither polyphosphate nor carbonate particles within these films are able to scatter light by themselves, so that we should assign the large film reflectivity to hollow structures formed by these particles [12–15].

Fig. 2 shows an electron scanning micrograph and the corresponding P, Al and Ca mappings of D3 film. In films D3, D5 and D8 we observed flat structures with typical dimensions between 30 and 50 μm distributed over a matrix of elements of smaller dimensions (3 to 5 μm), which contains many voids. These flat regions are richer in Ca than in Al, while P is more homogeneously distributed throughout the sample. This shows that there is exchange of aluminium ions with calcium ions around the polyphosphate chains in these regions.

We obtained TEM micrographs of a powder mixture of polyphosphate and carbonate ($Al[PO_3]_n/CaCO_3 = 60:40$). Fig. 3a shows a brightfield image of large aggregates with irregular morphology. Darkfield micrographs, Fig. 3b, c and d, are from the images obtained using diffracted electrons but at different positions of the lens aperture. The images show many brilliant spots that are assigned to small $CaCO_3$ crystals scattered over clear (but not brilliant) massive particles. These are non-crystalline but display some anisotropy, since they have a weak ability for electron diffraction. Upon subjecting the samples to an intense electron beam, these also undergo shape changes, showing the formation of bubbles associated with the volatilization of water within the particles. This is analogous to hollow particles formation described in [15].

For the sample with the greatest polyphosphate concentration ($Al[PO_3]_n/CaCO_3 = 80:20$) (Fig. 4)

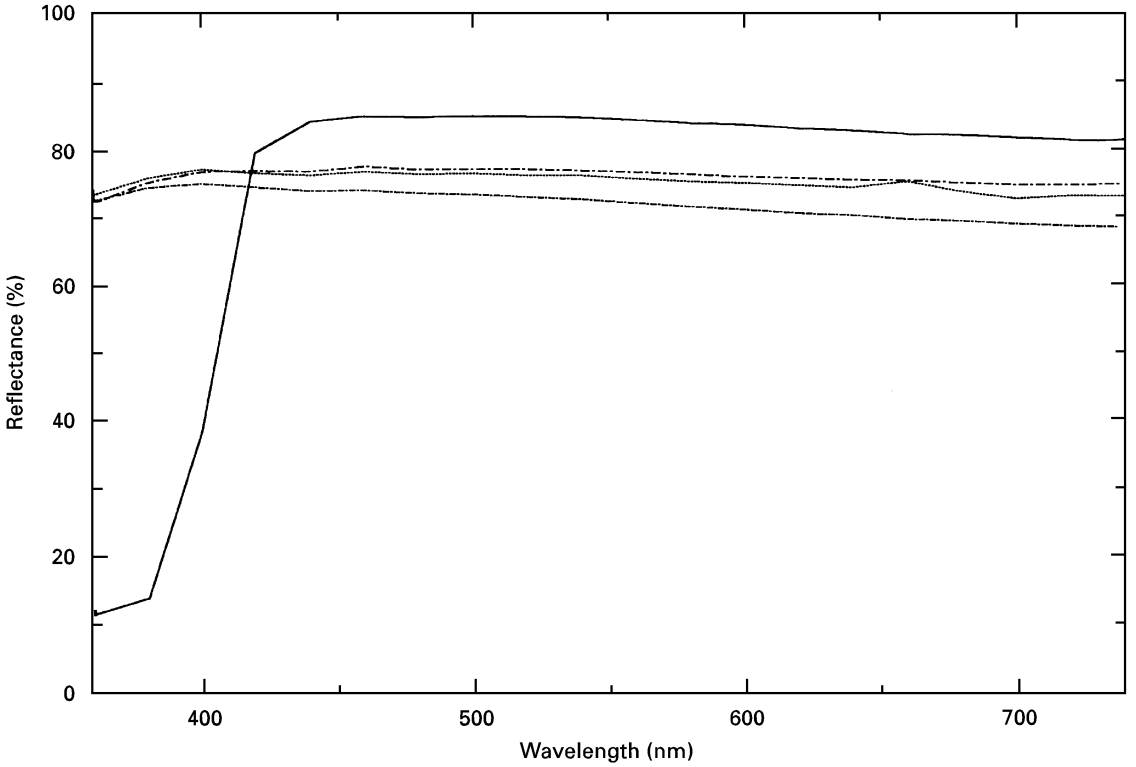

Figure 1 Diffuse reflectance spectra of films D3 (-·····-), D4 (- - -), D6 (····) and standard TiO_2/PVA (———).

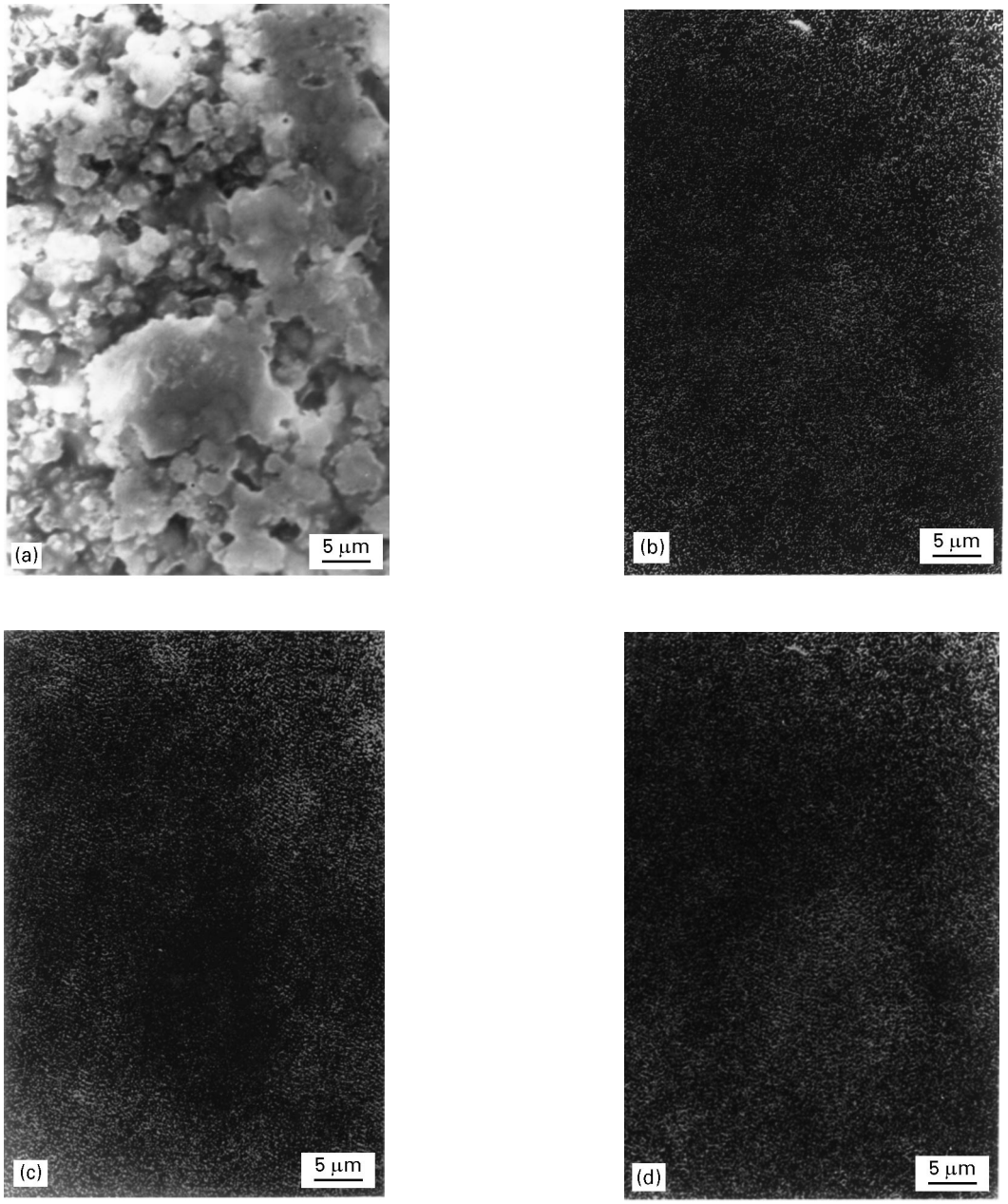

Figure 2 (a) Scanning electron micrograph and (b) the P, (c) A1 and (d) Ca mappings of film D3. Scale bar = 5 μm.

this phenomenon is so intense that we could not obtain a micrograph from an undamaged sample, even using low-intensity beams.

X-ray diffractograms for PVA resin dry films, containing powdered aluminium polyphosphate and calcium carbonate, either separately or admixed confirm that there is a chemical reaction between the two inorganic solids during film casting. The diffractograms of isolated pigments and polymer (both as powders or within PVA films) show the same behaviour, i.e. a typical amorphous halo in the case of polyphosphate and PVA and the calcite diffractogram in the case of carbonate [16]. Fig. 5 presents X-ray diffractograms of films containing both $Al[PO_3]_n$ and a $CaCO_3$ which were compared with their standards. We observe a decrease in carbonate peak intensities (relative to each film standard) as the polyphosphate concentration is increased, which is evidence for the consumption of calcium carbonate. We did not observe significant changes in the positions of the diffractogram peaks or the appearance of new peaks, which indicate that the unreacted calcium carbonate remains in its original crystalline form and that the reaction product formed *in situ* precipitates as a non-crystalline solid.

The tunnelling images of films from sample D5 and the respective controls are shown in Fig. 6. In the polyphosphate–PVA film we observe an oriented array of the inorganic particles. In this case, it seems that all the original polyphosphate particles are connected to each other as if they are welded. This result is unexpected for a film made entirely of dispersed amorphous solids, but it can be understood as a result of mutual influence of the organic matrix and inorganic particles, which operates during film drying. In the film which contains carbonate and PVA, the structures seen in the micrograph are also oriented, but it is still possible to identify the original contours of the carbonate particles. Finally, film D5 (prepared with

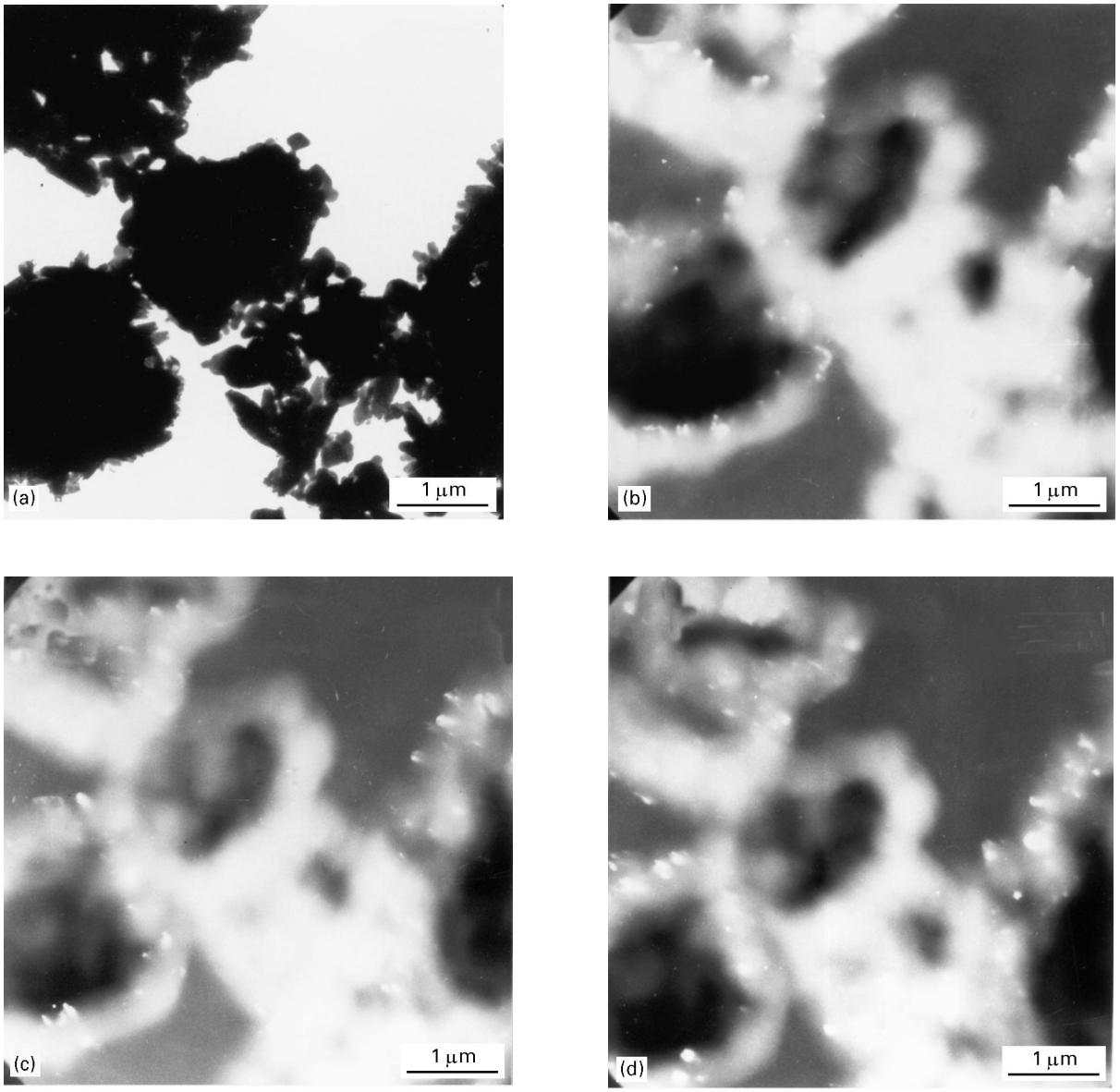

Figure 3 Transmission electron micrographs: (a) brightfield and (b), (c) and (d) darkfield images of powder mixtures of aluminium polyphosphate and calcium carbonate ($Al[PO_3]_3/CaCO_3 = 60:40$ volume). Scale bar = 1 μm.

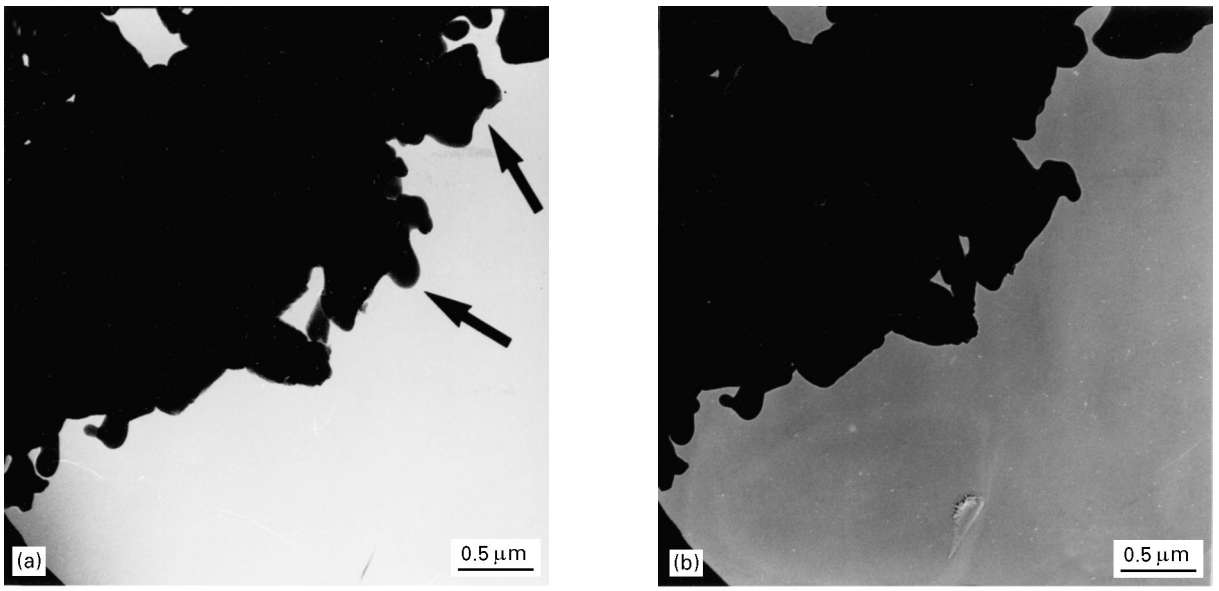

Figure 4 Transmission electron micrographs of a mixture of aluminium polyphosphate and calcium carbonate ($Al[PO_3]_3/CaCO_3 = 80:20$ volume), taken at two consecutive times: (a) was obtained prior to (b), within the same field. Some major morphological changes are indicated by the arrows. Scale bar = 0.5 μm.

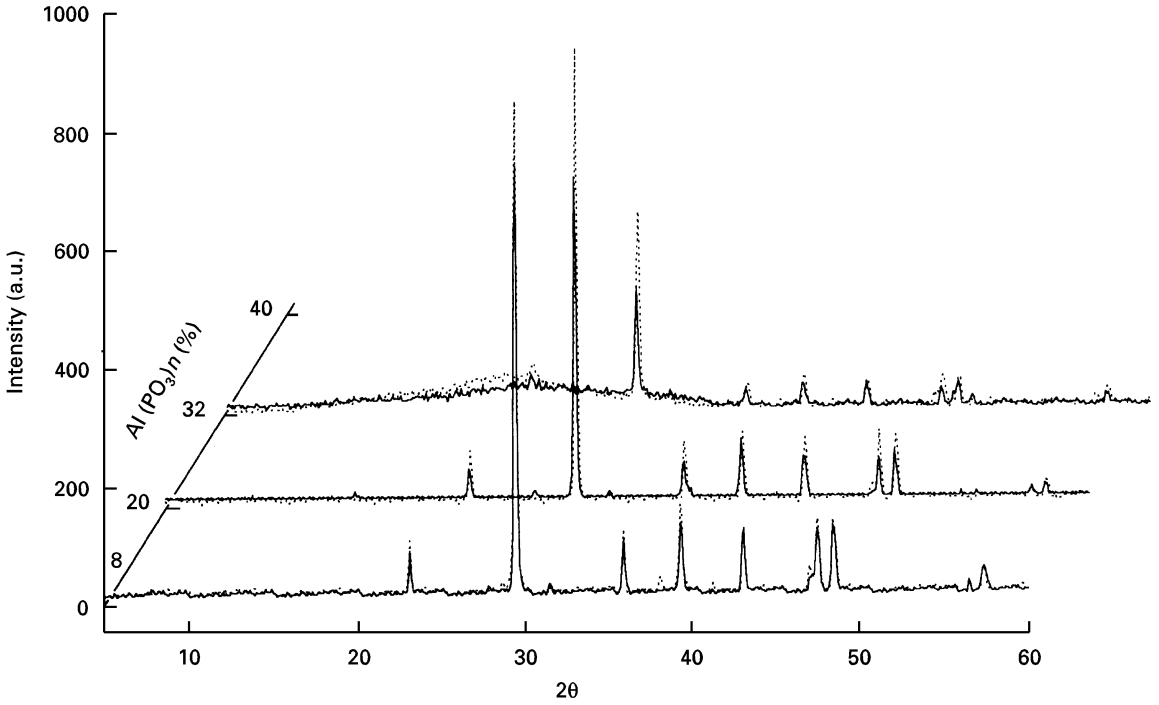

Figure 5 X-ray diffractograms of films D1, D4 and D7 (———) and their respective standards (····). Standards contain $CaCO_3$ and PVA, only.

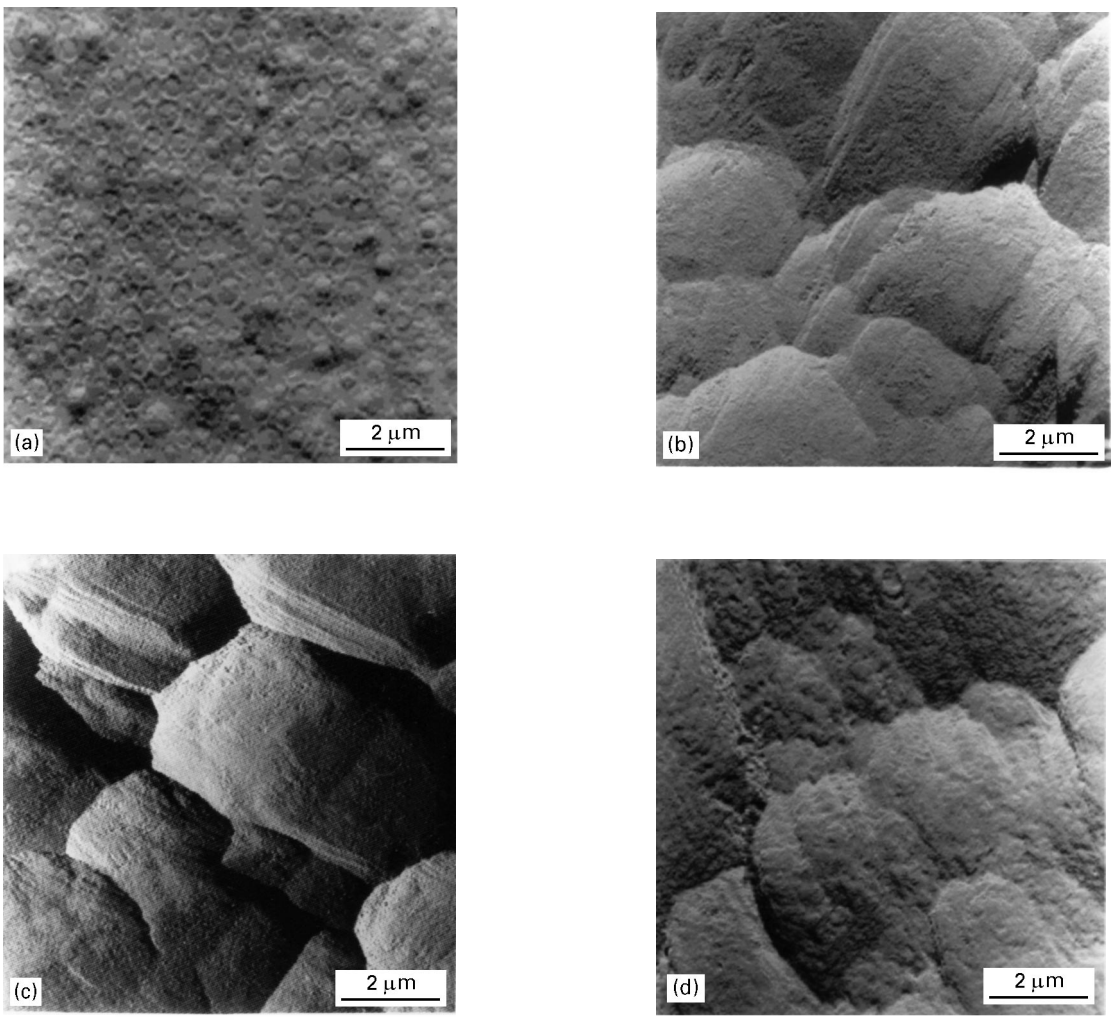

Figure 6 Atomic force image of (a) film with pure PVA, (b) tunnelling images of films with polyphosphate/PVA, (c) PVA/carbonate and (d) D5. Scale bar = 2 μm.

polyphosphate, carbonate and PVA) shows regions with a similar morphology as observed in the film made with polyphosphate and PVA only. D5 displays considerable small-scale roughness as compared to the film without carbonate. Height differences are smaller in the absence of carbonate, closely resembling the regions identified as the flat plates, observed in the SEM.

The results presented show that the hollow and flat structures are formed within films made with polyphosphate, carbonate and PVA. Given the dimensions of these structures, these may be held responsible for the light-scattering ability of these films.

The colloidal dispersions of aluminium polyphosphate, calcium carbonate and polymer lattices are in some way similar to those found in biological systems. They have a macromolecular component and reactive inorganic material within an aqueous environment, which are the essential prerequisites for processes analogous to supramolecular pre-organization and interfacial molecular recognition. For this reason, we propose the following model, to describe the process of film opacification.

(i) While the film is drying, the resin particles in the dispersion aggregate and coalesce forming a tridimensional network.

(ii) This polymeric network has some domains filled with polyphosphate and carbonate particles still surrounded by water. In these regions, the water allows chemical reaction by dissolution and reprecipitation of the inorganic compounds, so that crystalline calcium carbonate and amorphous aluminium polyphosphate react to form a non-crystalline (or mesophasic) mixed calcium–aluminium carbonatophosphate.

(iii) As drying proceeds, the swollen particle surfaces dry faster than the bulk and become more rigid than their interior. By the end of the drying process, the rigid particle surfaces are also bound to the highly viscous polymeric matrix so that the volume contraction caused by water loss requires the formation of voids or hollow structures within the film.

Recently, modern concepts of solid-state chemistry have enlarged the possibility of applications of phosphates as high technology materials because of their magnetic, transport, luminescent, optical and nonlinear properties [15, 17–19]. The approach described in this work may enlarge the array of techniques available for the preparation of phosphate materials designed for these properties.

4. Conclusions

Hollow and flat structures formed within coating films prepared with aluminium polyphosphate, calcium carbonate and PVA latex are responsible for their strong light backscattering ability. These structures are formed as the result of dispersion, chemical reaction and orientation of solid particles of polyphosphate and carbonate within the polymer network during the film drying process.

Molecular tectonic principles are applicable to a system with a large concentration of both amorphous and crystalline, reactive solid particles, yielding materials with the desired morphologies (void domains sizes) and optical (coating) properties.

Acknowledgements

The authors are grateful to Dr Omar Teschke, Dr Mauricio U. Kleinke and Luiz L. Bonugli from the Physics Institute – UNICAMP for the STM/AFM images. The support of FAPESP and FINEP (Brazil) is gratefully acknowledged. EFS is a postdoctoral fellow from CNPq.

References

1. S. MANN and P. CALVERT, *J. Mater. Sci.* **23** (1988) 3801.
2. A. H. HEUER, D. J. FINK, V. J. LARAIA, J. L. ARIAS, P. D. CALVERT, K. KENDALL, G. L. MESSING, J. BLACKWELL, P. C. REIKE, D. H. THOMPSON, A. P. WHEELER, A. VEIS and A. I. CAPLAN, *Science* **255** (1992) 1098.
3. S. MANN, *Nature* **365** (1993) 499.
4. *Idem*, *ibid.* **332** (1993) 119.
5. A. MONNIER, F. SCHÜTH, Q. HUO, D. KUMAR, D. MARGOLESE, R. S. MAXWELL, G. D. STUCKY, M. KRISHNAMURTY, P. PETROFF, A. FIROUZI, M. JANICKE and B. F. CHMELKA, *Science* **261** (1993) 1299.
6. S. MANN, D. D. ARCHIBALD, J. M. DIDYMUS, T. DOUGLAS, B. R. HEYWOOD, F. C. MELDRUM and N. J. REEVES, *ibid.* **261** (1993) 1286.
7. D. WALSH, J. D. HOPWOOD and S. MANN, *ibid.* **264** (1994) 1576.
8. B. R. HEYWOOD and S. MANN, *Langmuir* **8** (1992) 1492.
9. *Idem*, *J. Amer. Chem. Soc.* **114** (1992) 4681.
10. P. A. BIANCONI, J. LIN and A. R. STRZELECKI, *Nature* **349** (1991) 315.
11. B. C. BUNKER, P. C. RIEKE, B. J. TARASEVICH, A. A. CAMPBELL, G. E. FRYXELL, G. L. GRAFF, L. SONG, J. LIU, J. W. VIRDEN and G. L. MCVAY, *Science* **264** (1994) 48.
12. M. KERKER, "The Scattering of Light and Other Electromagnetic Radiation" (Academic Press, New York, 1969).
13. R. WEAST and M. J. ASTLE (eds) "CRC Handbook of Chemistry and Physics" (CRC Press, Boca Raton, 1980).
14. J. BRANDRUP and E. H. IMMERGUT (eds) "Polymer Handbook" (John Wiley, New York, 1975).
15. E. C. O. LIMA and F. GALEMBECK, *Colloids Surf. A* **74** (1993) 65.
16. Joint committee on powder diffraction standard, "Powder Diffraction File 1973, Search Manual-Alphabetical Listing – Inorganic Compounds" (JCOPDS, Swarthmore, 1973).
17. J.J. VIDEAU and V. DUPUIS, *Eur. J. Solid State Inorg. Chem.* **28** (1991) 303.
18. G. LE FLEM, *ibid.* **28** (1991) 3.
19. P. P. ABREU FILHO, F. GALEMBECK, F. C. G. GANDRA, M. L. BAESSO, E. C. SILVA and H. VARGAS, *Langmuir* **6** (1990) 1013.

Received 6 March 1995
and accepted 17 September 1996